



Synthesis of iron-based nanoparticles and comparison of their catalytic activity for degradation of phenolic waste water in a small-scale batch reactor

Avik De^b, Asim K. De^{a,*}, Gouri Sankar Panda^b, Sandip Haldar^c

^aDepartment of Chemical Engineering, University of Calcutta, 92, A.P.C Road, Kolkata 700009, India, Tel. +91 9477203215; Fax: +91 3323519755; email: akdecuce@yahoo.com

^bDepartment of Chemistry, Asansol Engineering College, Vivekananda Sarani, Kanyapur, Asansol 713305, India, emails: de.avik1986@gmail.com (A. De), p_gouri@yahoo.com (G.S. Panda)

^cDepartment of Physics, Asansol Engineering College, Vivekananda Sarani, Kanyapur, Asansol 713305, India, email: sand_ju@yahoo.com

Received 6 October 2015; Accepted 22 January 2016

ABSTRACT

In the present work, iron-based nanoparticles were synthesized by sol–gel method (iron oxide I), modified co-precipitation method (iron oxide II), reduction of FeSO₄ by NaBH₄ (nano zero-valent iron I, nZVI I), and reduction of FeSO₄ by NaBH₄ in presence of chelating ligand EDTA (nZVI II) for use as a catalyst for degradation of phenol. Particle characterization was performed for each set of samples by UV–vis spectra, X-ray diffraction, Fourier transformed infrared spectroscopy (FTIR), dynamic light scattering (DLS), and field emission scanning electron microscopy (FESEM). FESEM was performed with iron oxide II and particle size was found to be 36.5 nm. The average particle diameter obtained for nZVI was in the range of 141–150 nm. nZVI(II) has been found to be most efficient with respect to high percentage degradation of phenol in an hour under optimum operating condition at room temperature which were as follows: catalyst concentration = 0.05 g/l, pH 3, phenol:hydrogen peroxide (50%) concentration = 1:14 (stoichiometric ratio), temperature = ambient. Brunauer–Emmett–Teller (BET) surface area measurement also showed higher surface area for nano zero-valent iron (nZVI) particles than compared to other iron oxides. The initial phenol concentration was varied in the range of 50–400 mg/l. Degradation efficiency was found decreasing with increasing initial concentration of phenol. Iron oxide I and II can be successfully recovered and reused.

Keywords: Iron nanoparticle synthesis; Characterization; Comparison among catalysts; Heterogeneous Fenton's process; Phenol degradation; COD reduction

1. Introduction

Wastewater treatment using advanced oxidation processes (AOPs) has been of enormous importance for the last two decades. Also, degradation of persistent organic pollutants is posing a tremendous

challenge to environmental scientists as the environmental rules and regulations are becoming more and more stringent these days. According to the US EPA as well as Indian environmental regulations, phenol and its derivatives are in the priority pollutants list due to their recalcitrant properties and high toxicity toward common microbial flora [1]. Environmental

*Corresponding author.

technologists are working hard in finding a commercially viable solution to get rid of the unavoidable industrial menace.

Among various AOP, Fenton's reagent being a widely studied process was utilized for removal of organic pollutants during last two decades [2]. Though Fenton's reagent is a highly popular process to deal with such pollutants due its *prima facie* apparent cost effectiveness, it however suffers from serious disadvantages like generation of colloidal iron containing precipitates, low TOC conversions, high sludge formation, and resulting low pH values. Moreover, separation of these colloidal precipitates warrants for additional processing like coagulation, neutralization, sedimentation, and filtration which in turn increases ultimate operational cost [3].

Hence, an alternative technology is much in demand ensuring easy separation of catalysts from the reaction medium. Consequently, heterogeneous catalysis is becoming more and more popular than those so-called catalytic wet hydrogen peroxide oxidation processes. As a solution iron-based nanocatalysts might be suitably tried. Study of related literatures reveal that phenol, a toxic water pollutant can be effectively degraded in presence of iron oxide minerals [4,5]. Decomposition of hydrogen peroxide and subsequent degradation of pollutants depend upon the specific characteristic of the iron oxide [5,6]. Great variation and structural chemistry variability of iron oxides is attributed to two oxidation states of iron i.e. ferrous and ferric variety in a wide range of pH and condensation reaction [3]. Different chemical methods are now in wide use for the synthesis of iron oxide nanoparticles. Synthesis of iron oxide nanoparticles mostly suffers from two types of complexity [7,8]; (1) Colloidal nature of the iron oxides nanoparticles. (2) Nonexistence of a reproducible and cost effective process for commercialization avoiding complications in purification. In depth study of literatures reveal great variation in the methods of preparation of iron oxide nanoparticles even though prepared through a particular route. This may be due to difficulty encountered in getting mono-dispersed population of magnetic particles of suitable size. Naturally, a reproducible and cost-effective process is in demand for commercial preparation of nanoparticles avoiding process complications. Although this method provided hydrophilic nanoparticles with poor control over size, core crystallinity, and size dispersity of the nanoparticles, but the synthesis is environment-friendly in nature due to absence of any hazardous organic solvent or any bio recalcitrant polymer made capping agent.

It is an established fact that effectiveness of catalysts depend on the surface area of the participating

catalysts. However, a recent study has claimed that in case of iron oxide nanocatalysts, particle crystallinity is a major factor behind the effectiveness of nanocatalysts compared to surface area [8]. Previous workers like Valentine and Wang compared different iron oxides catalysts [5] and Huang et al. [4] also compared efficacy of various iron oxides for the degradation of 2-chlorophenol, but comparison between methods of preparation of iron oxides at varying room temperatures are not yet investigated. Also no report of comparison between the prepared nano iron oxide with zero-valent iron particle for the degradation of phenol is available. Here, in our study we prepared samples containing iron nanoparticles under four room temperature conditions of which two were based on iron oxide and other two were zero-valent iron nanoparticles (nZVI). Graphs for optimization of parameters like pH, initial catalyst concentration and hydrogen peroxide additions were not shown in present work, since extensive work was previously carried out by several researchers in this area [6,9] and almost similar results as those of earlier workers were achieved by us. We put stress on the initial concentration of the pollutants to quantify phenol degradation. Certain modifications were carried out for eliminating complications in synthetic route. Reducing initial catalyst load up to 10 times compared to related literature [6] was one of them. Nanoparticles synthesized by reduction of FeSO_4 by NaBH_4 (nZVI) resulted most effective catalyst. After characterization, those catalysts were used for degradation of model pollutant phenol.

Other important aspects of the present work included selection of harmless or innocuous organic chemicals in the synthesis and adoption of environment-friendly methodology resulting in reproducible values. Accepting particle agglomeration as a natural corollary in a water base method; considering green chemistry it is widely popular among scientists as water-based approaches for abatement of pollution are generally environment-friendly in nature.

2. Materials and methods

2.1. Chemicals

The following chemicals of E. Merck (India) AR grade were procured: ferric chloride hexa hydrate, ethyl alcohol, ferrous chloride tetrahydrate, phenol, sodium hydroxide, hydrochloric acid, sodium borohydrate, *n*-butanol. Iron nitrate nonahydrate, tetra ethyl ortho silicate, cerium(IV) sulfate procured were of AR grade E. Merck Germany. Double-distilled water was used purchased from National Chemical Company. All chemicals were used in received conditions.

2.2. Instruments

X-ray diffraction (XRD) analysis was performed by: PANalytical Machine Model No. PW.3040/60.

Fourier transformed infrared spectroscopy (FTIR) analysis was done by Thermo Scientific Nicolet iS5 iD3 attenuated Total Reflectance model. Particle size and Zeta potential determination of the dispersed nanoparticle was performed by Malvern particle size analyzer (Zetasizer). Phenol degradation was monitored by Perkin Elmer UV–vis data recording spectrophotometer.

GC analysis was performed Bruker GC-450, column = CP SIL 8CB with FID detector. The overall operating program is shown in Table 1.

Field emission scanning electron microscopy (FESEM) was performed by JEOL-ZSN-7600S-FESEM. COD reduction monitored by closed reflux method by the help of a Merck programmable digester (APHA, 6th Edition). BET surface area was measured by Nova 1000C Quant chrome analyzers. Initial and residual H_2O_2 concentration was measured by Ceric(IV) sulfate method [10].

2.3. Preparation of nanoparticle catalysts through different methods

Co-precipitation method [11] was applied to prepare iron oxide nanoparticles by initially mixing 2 g of $FeCl_2$ and 5.4 g of hydrated $FeCl_3$ in 300-ml hot water in which 5.0 g of sodium hydroxide was added with constant stirring. The process was modified during final stage. The precipitated mass was washed with water and high purity ethanol and finally dried in a vacuum hot air oven.

Fe_3O_4 nanoparticle was prepared by co-precipitation method where purging of inert gas like nitrogen was not done. Instead, all the solutions are boiled and cooled for two hours to remove dissolved oxygen during preparation phase. Similar process was reported in the literature [12].

nZVI was prepared by reducing 30 g of Fe(II) sulfate in 400-ml double-distilled water by sodium borohydride ($NaBH_4$) solution (8 g in 400 ml), in oxygen-free medium. Nitrogen gas was purged during

the synthesis stage with a nominal flow rate. $NaBH_4$ was kept excess in order to ensure complete reduction. Almost similar process was done by other researchers without purging nitrogen gas [13]. Yield was nearly 70%. During preparation, 25% NH_4OH was added to increase percentage yield. In a modified way, nZVI was also prepared by adding complexing or chelating ligand Na_2EDTA which is air stable in nature [14]. Iron content of the synthesized nZVI and air stable nZVI was measured by standard volumetric method [15].

Before the reaction, phenol adsorption reaction was tested with synthesized nanoparticle and no significant (below 5%) phenol depletion occurs in this case.

2.4. Phenol degradation experiments

Batch experiments were carried out at ambient temperature in 250-ml glass beaker having magnetic stirrer and 100-ml synthetic waste water with initial concentration of 100–400 mg/l was added. Initial catalyst concentration (Iron oxide I, II and nZVI I, II) was kept 0.05 g/l. The beaker was covered with a black container to avoid photodegradation. Nanoparticles were added directly to the reaction mixture and sonicated for half an hour. During sonication, temperature of the sonicator bath may raise 1–2°C which was ignored in this study. The reaction was then started by adding 972 mg/l or 28.58 mM H_2O_2 and it was added all at once. pH of the reaction mixture was adjusted either by 0.1 N H_2SO_4 or 0.1 N NaOH. Phenol degradation was monitored spectrophotometrically following 4-amino antipyrine method [16]. Phenol conversion was also studied by gas chromatographic method having less chance of inorganic radical interference.

Samples were drawn from reaction mixture and the reaction was ceased by adding *n*-butanol as a hydroxyl radical scavenger; otherwise hydrogen peroxide will generate more hydroxyl free radicals that will drive the reaction forward. After that it was centrifuged with the help of a (Remi RT 24 Research Centrifuge) at 10,000 rpm for 10 min to separate nanoparticles. Nanocatalysts so used were recovered by centrifugation and second batch of experiments were taken up with same initial phenol concentration keeping other conditions unaltered. Experiments with nZVI were carried out in two ways. Soluble iron concentration was determined by 1,10-phenanthroline method [17]. All the experiments were repeated thrice.

Table 1
Temperature program of the oven

Rate (celcius/min)	Temp. (°C)	Time (min)
Initial	40	3
15	130	2

3. Results and discussions

3.1. FTIR study

An FTIR spectrum of the Iron oxide prepared by sol-gel method and modified co-precipitation method was taken. FT-IR spectrum of nZVI I revealed abroad spectrum at $3,445.63\text{ cm}^{-1}$ and it can be assigned to the stretching modes of surface H_2O molecules or may be an envelope of hydrogen bonded surface OH groups [18]. The absence of strong band at $3,144\text{ cm}^{-1}$ excludes the presence of goethite structure at the formation phase. The IR band at $1,639.19\text{ cm}^{-1}$ is close to the position of H_2O bending vibrations. The presence of a peak at 545 cm^{-1} is indication of Hematite phase [19]. Hematite spheres showed IR bands at 575, 485, 385, and 360 cm^{-1} . Aggregation as well as matrix effects, and also the crystallinity effect on the IR spectrum of hematite, were also reported in the present work. FTIR spectra of nZVI(II) where clear peak observed at $3,346\text{ cm}^{-1}$. This is due to partial oxidation of surface iron to $\gamma\text{-FeOOH}$ (lepidocrocite) [13].

3.2. XRD analysis

XRD pattern of the iron oxide sample prepared by modifying the sol-gel method was recorded where peak broadening revealed the amorphous nature of the sample (Fig. 1).

Iron oxide dried samples were analyzed by XRD analysis. Samples were divided into two parts; one part was calcined at 400°C for two hours, other remains same. Powder XRD was performed with the sample prepared by co-precipitation method which was mostly magnetite (Fe_3O_4) in nature according to JCPDS file no. 19-0629, which is shown in Figs. 2 and

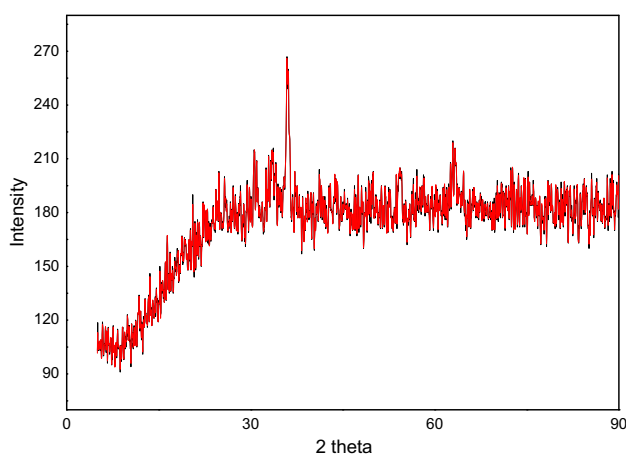
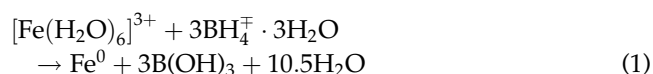


Fig. 1. XRD pattern of iron oxide prepared by sol-gel method.

3. An additional peak was observed for calcined substance which may be due to mixed phase formation (Fe_2O_3 along with hematite). Similar results were reported in the literature [8]. It is shown in Figs. 2 and 3.

nZVI prepared by the above-mentioned method also underwent XRD analysis where multiple peaks were observed due to rapid aerial oxidation of reactive zero-valent iron shown in Fig. 3.

The strong peak near $2\theta = 39^\circ$ and small peak near $2\theta = 65^\circ$ symbolizes partial formation of nZVI by the following reaction along with FeOOH (iron oxyhydroxide) phase. This is compatible with JCPDS file no. 44-1415 and 34-0529. The reaction is as follows:



XRD pattern of nZV(II) is shown in Fig. 4 where peaks are observed at 35, 54 and 64° .

3.3. Particle size analysis by DLS method and zeta potential measurement

This was carried out by Malvern nanoscale Zetaziser version 6.0. Three samples from each category of nanoparticle of different dilutions were investigated for determining particle size as well as zeta potential. The particle size distribution along with zeta potential value of nanoscale Fe_2O_3 , ZVI was shown in Figs. 5–7. The zeta potential value of nanoparticle dispersion is a good indicator of its aqueous phase stability. A colloidal system is generally stable if its zeta potential is higher than $+30\text{ mV}$ or less than -30 mV . For iron oxide II (Fe_2O_3), zeta potential value is 29.8 mV which indicates better stability in aqueous phase. Hydrodynamic diameter recorded was 236 nm .

For nZVI(II) the zeta potential was found to be -6.71 mV and hydrodynamic diameter is nearly $1,170\text{ nm}$ (Figs. 6 and 7).

The low stability of zero-valent iron nanoparticle may be the reason behind larger particle diameter [20]. Ionic strength of the medium as well as sonication time may be a factor for the particle stability which were not investigated in the present work.

3.4. FESEM analysis

FESEM was performed for the iron oxide sample prepared by modified co-precipitation method where magnetite phase formation was strongly recommended according to XRD and FTIR analysis; although Ferrihydrite ($\text{Fe}_5\text{HO}_8 \cdot 4\text{H}_2\text{O}$) may be

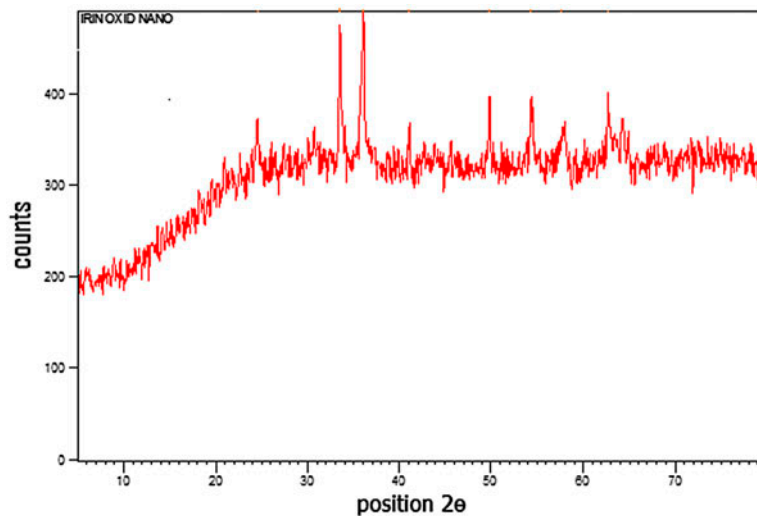


Fig. 2. XRD pattern of iron oxide prepared by modified co-precipitation method (before heat treatment).

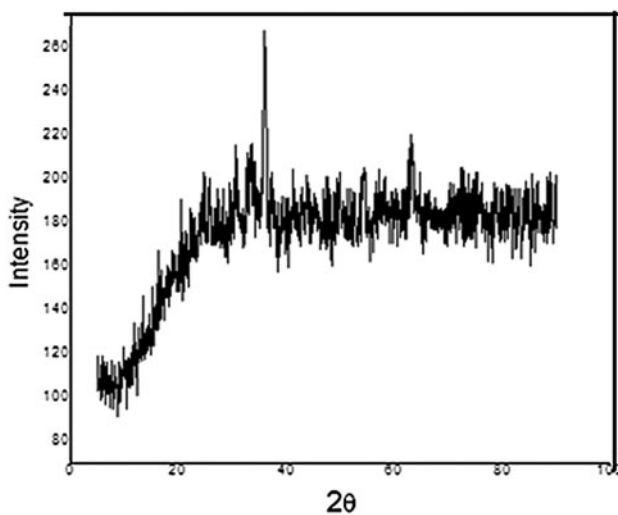


Fig. 3. XRD pattern of iron oxide prepared by modified co-precipitation method (after heat treatment).

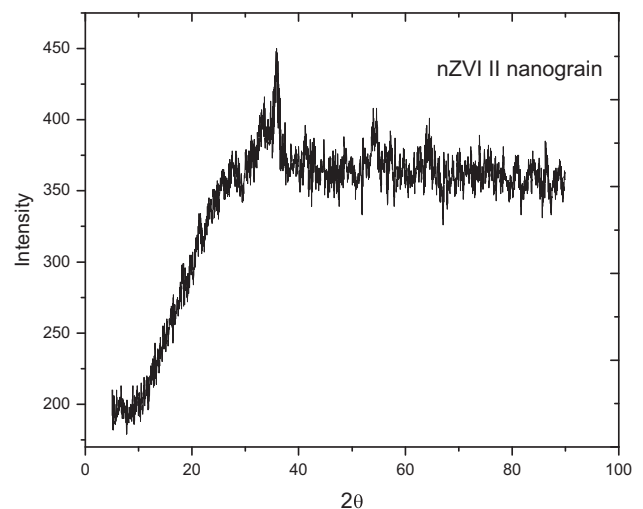


Fig. 4. XRD pattern of nZVI(I) prepared by FeSO_4 reduction method.

considered as a precursor of magnetite formation [21]. Photographs of different view of the sample solution have been taken by JEOL instruments to elucidate average particle size. Magnetite particles are spherical in shape and have a very strong tendency to aggregate which can form larger particles as shown in Fig. 8. Similarly, micrographs of modified nZVI or nZVI(II) were taken where nanoparticles clusters are obtained with average particle size of 141 nm. Again particles were found in agglomerated form as shown in Fig. 9.

The agglomerated form clearly revealed by the FESEM micrographs. The average particle size obtained was 36.5 nm. It has been observed that at pH

7.0 agglomerations are particularly strong, since the repulsive forces between the particles are negligible. Similarly, nZVI aggregate was also observed by Taha and Ibrahim [22]. Furthermore, in the case of magnetic particles, the agglomeration is enhanced by magnetic-dipole interactions [23]. Therefore, it can be assumed that the catalyst suspension consists mainly of agglomerates rather than of primary nanoparticles.

3.5. BET surface area measurement

BET surface area measurement was performed by N_2 adsorption–desorption method at 77.4 K. It was

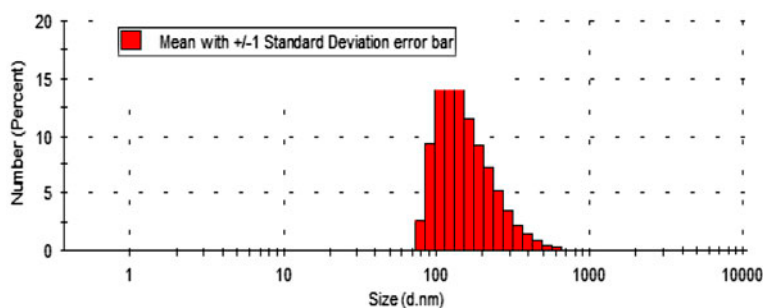


Fig. 5. Particle size determination of iron oxide(II).

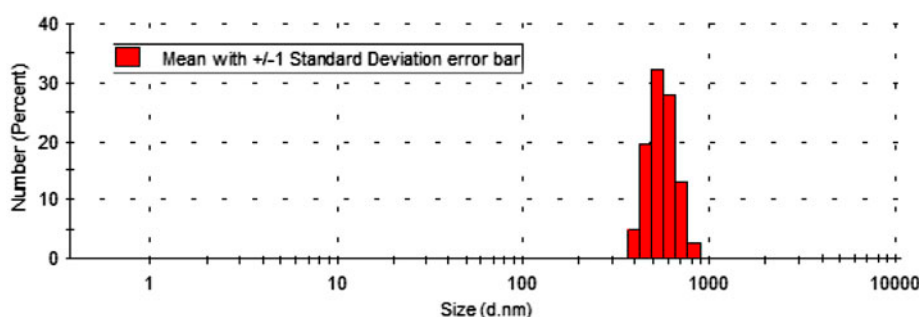


Fig. 6 Particle size distribution for nZVI(II).

observed that surface area for nZVI(II) was $225 \text{ m}^2/\text{g}$ whereas the corresponding figure for iron oxide(II) was found to be $30 \text{ m}^2/\text{g}$.

The details of characterization for iron nanoparticles are shown in Table 2.

3.6. Comparison between different Iron-based nanoparticles as catalysts

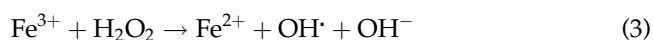
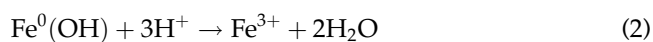
The degradation of Phenol and associated compounds depends on ring rupture of pollutants through oxidation which *inter alia* depends on generation of hydroxyl radicals. In all the cases stoichiometrically excess hydrogen peroxide was added to ensure rapid *in situ* generation of hydroxyl free radicals. These radicals come from decomposition of hydrogen peroxide on catalyst surface. Actually it involves radical chain reaction [4].

Iron oxide prepared from sol–gel method is mostly Fe_2O_3 along with little Fe. The particle crystallinity of iron-based nanoparticles depends on the duration and temperature of heat treatment. With increasing heat treatment temperature, particle nature undergoes changes from amorphous to crystalline state and is supported by corresponding XRD pattern obtained. Thermally induced sintering as well as growth of

nanoparticles are important parameters for exerting catalytic behavior. The relative content of amorphous Iron oxide with respect to crystalline nanograin depends on extent of calcination [20].

One of the major advantages of using Heterogeneous Fenton system using iron oxide nanoparticle is that the process can be carried out near neutral pH which is an important requirement for the water remediation technologies. But it is also reported that the catalytic process is relatively inefficient near neutral pH due to several competing reactions [21]. The decomposition of H_2O_2 catalyzed by iron oxide is a pH-dependent process and more accurately it is a modified Haber–Weiss mechanism according to Kitajima et al. [24] at neutral pH. It has been established that H_2O_2 decomposition in the presence of iron oxide can often be described by pseudo-first-order reaction [25].

In Fenton-type oxidation mechanism $\cdot\text{OH}$ free radical is generated in the presence of aqueous Fe^{2+} and more soluble ferrous iron is generated via the following mechanism as given by previous workers [3].



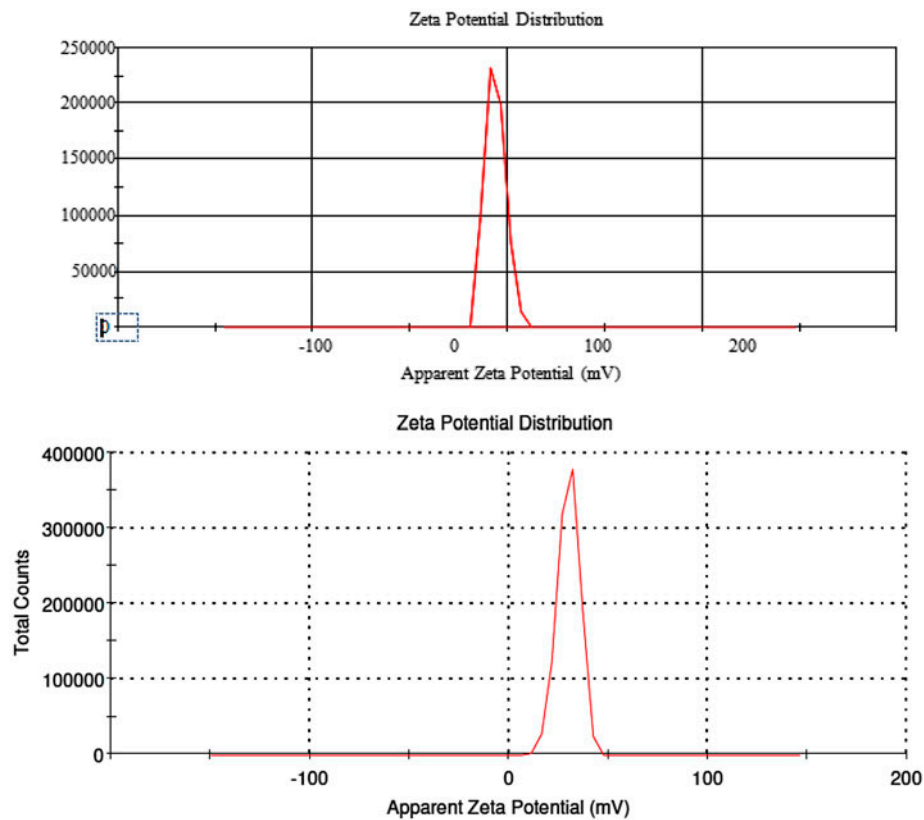


Fig. 7. Zeta potential of Fe₂O₃ and nZVI(II).

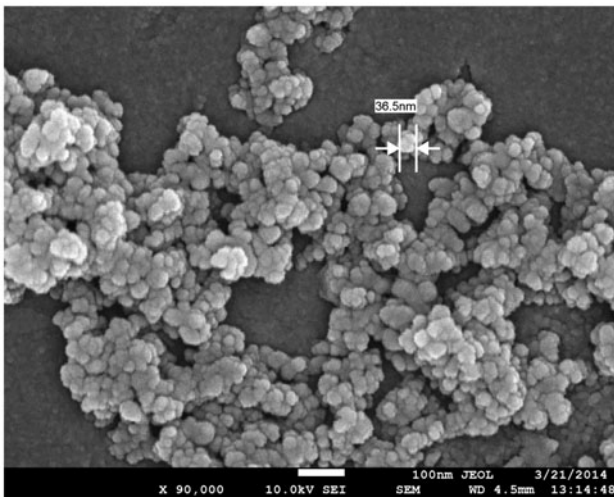


Fig. 8. FESEM image (morphology and size) of nanoparticle prepared by modified co-precipitation method.

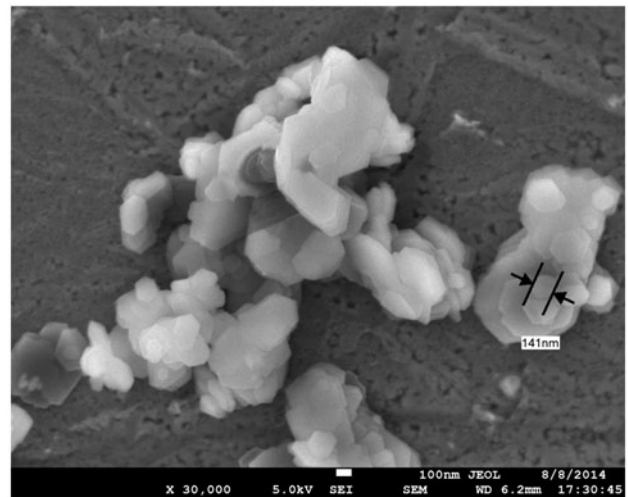


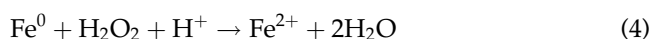
Fig. 9. FESEM image (morphology and size) of nZVI(II) nanoparticle.

The dissolution of nano iron oxide increases at lower pH value. The removal of ferric ion to the solution can initiate a chain of reaction which may start

homogenous Fenton-like reactions. The formation of hydroxyl free radical can be explained from the following reaction at comparatively high pH value.

Table 2
Characterization details of synthesized nanoparticles

Nature of the particle	UV–vis spectra (peak obtained at) nm	XRD (peak obtained w.r.t 2θ value)	DLS (avg hydrodynamic diameter)	FTIR (in cm^{-1}) (nature of the peak and corresponding wave number)	% Content of iron by volumetric method
Iron oxide(I)	220	25	>1,000 nm	1,654	34
Iron oxide (II)	255	36	236	1,718	56
nZVI(I)	230	45	>1,000 nm	1,107	89
nZVI(II)	397	36	1,170	3,346	91



Fe(IV) is an unstable species and a weaker oxidant [26]. The average particle size obtained from the above methods can be calculated either from Debye-Scherrer equation or directly from FESEM micrographs. It is also observed that particle size has a strong correlation with % conversion of phenol.

Initial concentration of Phenol was varied in the range of 50–400 mg/l. Initial nanocatalyst concentration was 0.05 g/l which was 10 times less compared to the concentration depicted elsewhere [9,26] and hydrogen peroxide (50%) having initial concentration of 28.58 mM was added. The stoichiometric ratio of Phenol oxidation is 1:14. Hence, depending on the initial Phenol concentration hydrogen peroxide was added to the reaction mixture to initiate the same. Zhang et al. claimed that too high H_2O_2 dose may inhibit the phenol degradation reaction [27]. Hence, experiments with higher dose of H_2O_2 were not performed. Other conditions were pH 2.5–3, temperature = 35 °C reaction volume = 100 ml. Maximum conversion of phenol using different nanocatalysts along with COD reduction, C/C_0 vs. time with four different initial concentrations of phenol with same nanocatalyst and C/C_0 vs. time for different nanocatalysts with same initial concentration of phenol are shown in Figs. 10–12, respectively.

Maximum degradation was obtained for nZVI as solid catalyst which is nearly 90% with initial Phenol concentration 50 mg/L and decreases with increasing initial phenol concentration up to 400 mg/L. This is achieved within 14 h from the beginning of the reaction.

Nanoparticle are used as a water purifying agent, iron-based nanoparticle offer a high specific surface area and for nZVI different properties are generated

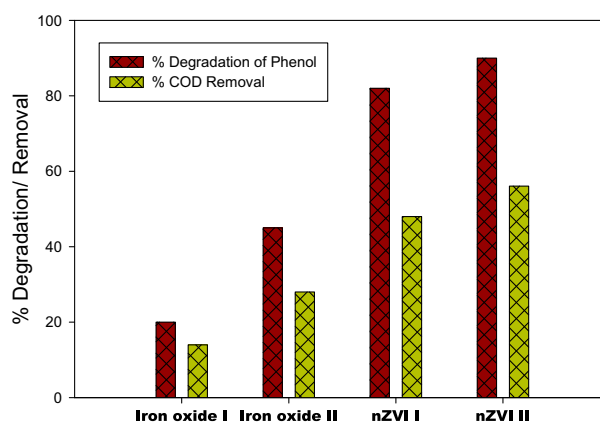


Fig. 10. Effect of nanoparticle type on phenol degradation and COD removal.

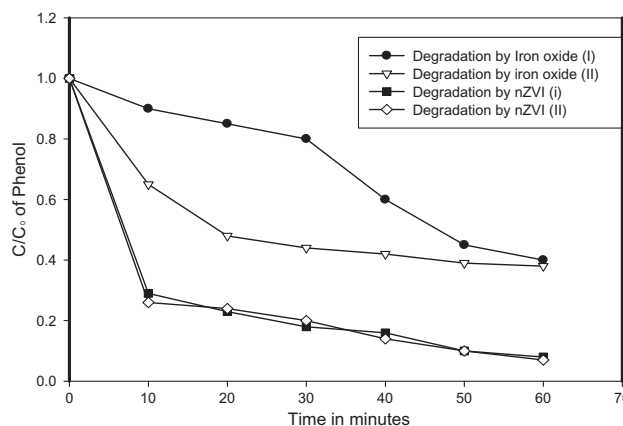


Fig. 11. Degradation of phenol with various iron-based nanocatalyst at pH 3, phenol: H_2O_2 = 1:14, temp. = ambient, reaction volume = 100 ml.

in comparison to their bulk properties which may lead to increase in catalytic properties [28]. Among the iron

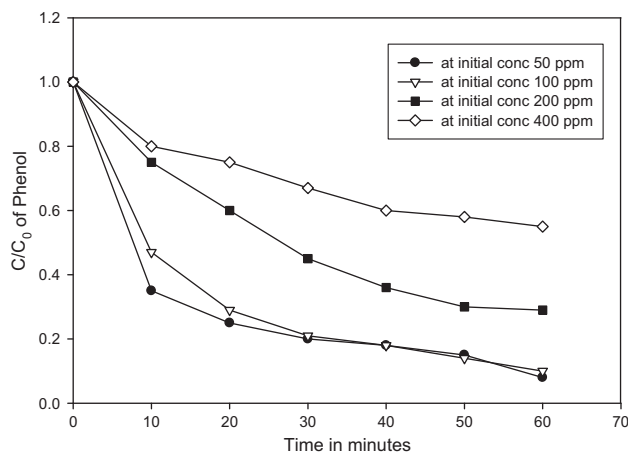


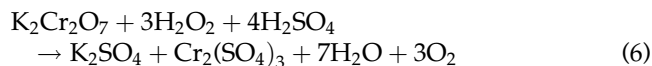
Fig. 12. Degradation of phenol with nZVI(II) taking various initial concentrations of phenol at pH 3, temp. = ambient, phenol: H₂O₂ = 1:14, reaction volume = 100 ml.

nanoparticle synthesized in solid state, nZVI gives the highest catalytic power in degrading phenol. It has been established by Radek Zboril et al. that catalytic efficiency does not depend on surface area of the catalyst, it rather depends on particle crystallinity. This could be one of the reasons along with high surface area (225 m²/g) due to which nZVI showed highest conversion effect compared to hematite nanoparticles which is clear from corresponding XRD pattern. The iron content in the iron oxide formed by sol-gel methods is nearly 38% due to the presence of silicon in resultant solid. This may be one of the reasons behind low reactivity. Further, it can be explained by core shell model of zero-valent iron nanoparticles according to which the mixed valence iron oxide shell is largely insoluble under neutral pH condition and it can protect the ZVI core from further oxidation [22,23]. Due to this reason pH of the aqueous solution must be shifted to acidic range so that sufficient amount of iron (as Fe²⁺) dissolution can be achieved [22]. It has been observed that maximum dissolution of the shell occurs at nearly pH 2 which is revealed from the degradation experiment performed. It was also supported by Taha and Ibrahim [22]. The presence of two nanoparticles in the core-shell structure may have profound impact on pollutant degradation where the metallic iron acts as the electron source like a reducing agent, while the oxide shell enhance sorption of contaminants via electrostatic interactions and surface complexation methods [23]. Surface area measurement also revealed that nZVI(II) has greater surface area compared to iron oxide which is reflected in its catalytic effect. Here, cumulative effect of surface quality and surface area was observed.

3.7. Phenol degradation and subsequent COD removal

In previous paper [2] we reported that during homogeneous Fenton reaction there is a steady change in color from colorless to brown then black and it is strongly correlated with overall degradation. But phenol degradation in presence of iron oxide nanocatalyst (heterogeneous Fenton type process) did not show any color change. Hence, it is realized that the degradation mainly has occurred on the porous site of the nanocatalyst according to Zhang et al. [29]. It reveals that degradation follow different pathway. In the present work, GC-MS analysis of the resultant liquid was not performed. All the degradation experiments performed revealed that phenol removal is more than 80% within half an hour but COD removal is less than 60%. It is already shown in Fig. 10.

It has been found that COD value of 1st sampling data is greater than zero minute value although COD reduction occurred after 24 h silent degradation. This is due to H₂O₂ interference during COD digestion [30] according to the following reaction:



The extent of H₂O₂ interference in COD analysis was proportional to the remaining H₂O₂ concentration at the moment of sampling from the reaction system as depicted by Lee et al. [30]. Corrected COD data were recorded while drawing the graphs.

3.8. Reuse of nanocatalyst

A series of experiment was conducted to investigate the catalytic behavior of virgin and recovered nano iron oxide (both 1 and 2) and nZVI (both 1 and 2). The results are summarized in Fig. 13. The reaction parameters were kept constant during the reused experiment. Three cycles were performed to monitor phenol degradation efficiency. After first cycle the virgin nanoparticles were separated by centrifugation and washed thoroughly with distilled water and acetone. Then they were dried in a vacuum desiccator. After that they were used in second catalytic run maintaining experimental conditions unaltered. It has been found that there was no substantial reduction in the catalytic property. To investigate nanoparticle stability during storing, catalytic reactions are carried out under optimum conditions in three successive weeks. Phenol degradation efficiency was reached up to 76.15% in the final cycle which is shown in Fig. 13. It highlights the application of this iron oxide(II)

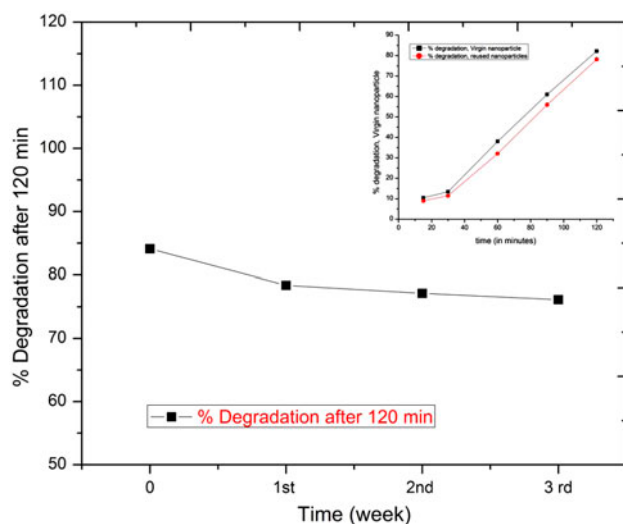
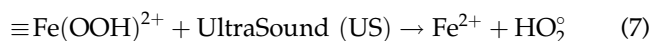


Fig. 13. Reuse of iron oxide nanocatalyst at various time intervals under optimized condition. Inset: % degradation of phenol with time by using virgin and reused nanoparticles.

nanoparticle in real-life wastewater treatment systems. Results regarding reuse of nZVI are not presented in this paper as sufficient amount of surface corrosion occurred due to low pH condition [31].

3.9. Effect of sonication

Compared to silent process ultra sound may play some role in overall phenol degradation mechanism. It is assumed that the limiting step in Fenton-like reactions is reduction of Fe(III) to Fe(II) mediated by Fe(OOH)²⁺ complex [32]. The dissociation of this complex is accelerated by sonication time and intensity. Production of active radicals may be enhanced by the following reactions:



4. Conclusion

Choice of catalyst is one of the important aspects of heterogeneous Fenton-type reaction and it is again confirmed by the present work. For low-cost environmentally benign treatment, catalyst generation at room temperature with cheaper nonhazardous reagents or

technique is required as explored in the present study. Not only the catalytic activity but also the stability of the catalyst is a crucial factor in heterogeneous Fenton-type reaction. In the present work, synthesized nanoparticles were found to be stable in terms of zeta potential measurement and reuse experiments. Among all the nanoparticles synthesized nZVI(II) gives the maximum phenol degradation (more than 90%) at low pH range but COD reduction is not satisfactory. Used oxide-based catalysts can be recovered and effectiveness measured up to three cycles. nZVI is difficult to recover as surface transition occurs at acidic pH. In future, stress will be given to maximize mineralization along with determination of probable reaction kinetics.

Acknowledgment

We convey our gratitude to Dr Dipankar Chakroborty, Department of Polymer Science and Technology, University of Calcutta for his help in carrying out FESEM and Dr Sampa Chakrobarti, Department of Chemical Engineering, University of Calcutta for allowing us to utilize her lab facilities. We also convey our deep gratitude to Mr Ranadhir Bhattacharya, Ex Scientific officer, BOC India Ltd for his help in language editing. We thank Asansol Engineering College & DST West Bengal for all sorts of financial and necessary help.

References

- [1] R. Anliker, Ecotoxicology of dyestuffs—A joint effort by industry, *Ecotoxicol. Environ. Saf.* 3(1) (1979) 59–74.
- [2] A.K. De, A. De, Role of color transformation during Fenton's oxidation of phenolic waste water in a large scale continuous stirred tank reactor (CSTR), *J. Indian Chem. Soc.* 5 (2013) 1–9.
- [3] A. Bach, A. Zach-Maor, R. Semiat, Characterization of iron oxide nanocatalyst in mineralization processes, *Desalination* 262 (2010) 15–20.
- [4] H. Hui Huang, M.C. Lu, J.N. Chen, Catalytic decomposition of hydrogen peroxide and 2-chloro phenol with iron oxides, *Water Res.* 35 (2001) 2291–2299.
- [5] R.L. Valentine, H.C. Ann Wang, Iron oxide surface catalyzed oxidation of quinoline by hydrogen peroxide, *J. Environ. Eng.* 124 (1998) 31–38.
- [6] N. Wang, L. Zhu, D. Wang, M. Wang, Z. Lin, H. Tang, Sono-assisted preparation of highly-efficient peroxidase-like Fe₃O₄ magnetic nanoparticles for catalytic removal of organic pollutants with H₂O₂, *Ultrason. Sonochem.* 17 (2010) 526–533.
- [7] S. Laurent, D. Forge, M. Port, A. Roch, C. Robic, L. Vander Elst, R.N. Muller, Magnetic iron oxide nanoparticles: Synthesis, stabilization, vectorization, physicochemical characterizations, and biological applications, *J. Chem. Rev.* 108(6) (2008) 2064–2110.

- [8] M. Hermanek, R. Zboril, I. Medrik, J. Pechousek, C. Gregor, Catalytic efficiency of iron(III) oxides in decomposition of hydrogen peroxide: Competition between the surface area and crystallinity of nanoparticles, *J. Am. Chem. Soc.* 129 (2007) 10929–10936.
- [9] Y. Shih, C. Hsu, Y. Su, Reduction of hexachlorobenzene by nanoscale zero-valent iron: Kinetics, pH effect, and degradation mechanism, *Sep. Purif. Technol.* 76 (2011) 268–274.
- [10] Manual, Determination of Hydrogen Peroxide and per Acetic Acid in Solution, Enviro Tech Chemical Services, Inorganic Chemicals Division, pp. 1–3. Available from: <<http://envirotech.com/pdf/PAA%20Analytical%20Method.pdf>>.
- [11] J.T. Lue, Physical properties of nanomaterials, encyclopedia of nano science and nanotechnology, in: H.S. Nalwa, vol. X, 2007, pp. 1–46. Available from: <www.aspbs.com/enn>.
- [12] A. Bandhu, S. Mukherjee, S. Acharya, S. Modak, S.K. Brahma, D. Das, P.K. Chakrabarti, Dynamic magnetic behaviour and Mössbauer effect measurements of magnetite nanoparticles using different chelating agents in the co-precipitation method, *Solid State Commun.* 149 (2009) 1790–1794.
- [13] M.B. Allabaksh, B.K. Mandal, M.K. Kesarla, K.S. Kumar, P.S. Reddy, Preparation of stable zero valent iron nanoparticles using different chelating agents, *J. Chem. Pharm. Res.* 2(5) (2010) 67–74.
- [14] Y.-P. Sun, X.-Q. Li, W.-X. Zhang, H. Paul Wang, A method for the preparation of stable dispersion of zero-valent iron nanoparticles, *Colloids Surf., A* 308 (2007) 60–66.
- [15] A.I. Vogel, *Quantitative Analysis*, sixth ed., Pearson Publication, London.
- [16] APHA (American Public Health Association), *Standard Methods for the Examination of Water and Wastewater*, 21st ed., American Public Health Association, Washington, DC, pp. 5–47.
- [17] APHA (American Public Health Association), *Standard Methods for the Examination of Water and Wastewater*, 21st ed., American Public Health Association, Washington, DC, 3.77.
- [18] M. Gotić, S. Music, Mössbauer, FT-IR and FESEM investigation of iron oxides precipitated from FeSO₄ solutions, *J. Mol. Struct.* 834–836 (2007) 445–453.
- [19] S. Musić, S. Krehula, S. Popović, Ž. Skoko, Some factors influencing forced hydrolysis of FeCl₃ solutions, *Mater. Lett.* 57 (2003) 1096–1102.
- [20] P.J. Vikesland, A.M. Heathcock, R.L. Rebodos, K.E. Makus, Particle size and aggregation effects on magnetite reactivity toward carbon tetrachloride, *Environ. Sci. Technol.* 41 (2007) 5277–5283.
- [21] M.C. Lu, J.-N. Chen, H.H. Huang, Role of goethite dissolution in the oxidation of 2-chlorophenol with hydrogen peroxide, *Chemosphere* 46 (2002) 131–136.
- [22] M.R. Taha, A.H. Ibrahim, Characterization of nano zero-valent iron (nZVI) and its application in sono-Fenton process to remove COD in palm oil mill effluent, *J. Environ. Chem. Eng.* 2 (2014) 1–8.
- [23] W. Yan, A.A. Herzing, C.J. Kiely, W.x. Zhang, Nanoscale zero-valent iron (nZVI): Aspects of the core-shell structure and reactions with inorganic species in water, *J. Contam. Hydrol.* 118 (2010) 96–104.
- [24] N. Kitajima, S. Fukuzumi, Y. Ono, Formation of superoxide ion during decomposition of hydrogen-peroxide on supported metal-oxides, *J. Phys. Chem.* 82(13) (1978) 10929–10936.
- [25] C. Gregor, M. Hermanek, D. Jancik, J. Pechousek, J. Filip, J. Hrbacand, R. Zboril, The effect of surface area and crystal structure on the catalytic efficiency of iron (III) oxide nanoparticles in hydrogen peroxide decomposition, *Eur. J. Inorg. Chem.* (2010) 2343–2351.
- [26] L. Xu, J. Wang, A heterogeneous Fenton-like system with nanoparticulate zero-valent iron for removal of 4-chloro-3-methyl phenol, *J. Hazard. Mater.* 186 (2011) 256–264.
- [27] J. Zhang, J. Zhuang, L. Gao, Y. Zhang, N. Gu, J. Feng, D. Yang, J. Zhu, X. Yan, Decomposing phenol by the hidden talent of ferromagnetic nanoparticles, *Chemosphere* 73 (2008) 1524–1528.
- [28] K. Rusevova, F.D. Kopinke, A. Georgi, Nano-sized magnetic iron oxides as catalysts for heterogeneous Fenton-like reactions—Influence of Fe(II)/Fe(III) ratio on catalytic performance, *J. Hazard. Mater.* 241–242 (2012) 433–440.
- [29] S. Zhang, X. Zhao, H. Niu, Y. Shi, Y. Cai, G. Jiang, Superparamagnetic Fe₃O₄ nanoparticles as catalysts for the catalytic oxidation of phenolic and aniline compounds, *J. Hazard. Mater.* 167 (2009) 560–566.
- [30] E. Lee, H. Lee, Y.K. Kim, K. Sohn, K. Lee, Hydrogen peroxide interference in chemical oxygen demand during ozone based advanced oxidation of anaerobically digested livestock wastewater, *Int. J. Environ. Sci. Technol.* 8(2) (2011) 381–388.
- [31] X. Zhang, Y.-m. Lin, X.-q. Shan, Z.-l. Chen, Degradation of 2,4,6-trinitrotoluene (TNT) from explosive wastewater using nanoscale zero-valent iron, *Chem. Eng. J.* 158 (2010) 566–570.
- [32] R. Molina, F. Martínez, J.A. Melero, D.H. Bremner, A.G. Chakinalab, Mineralization of phenol by a heterogeneous ultrasound/Fe-SBA-15/H₂O₂ process: Multivariate study by factorial design of experiments, *Appl. Catal. B: Environ.* 66 (2006) 198–207.